European Conference on Computational Fluid Dynamics
ECCOMAS CFD 2006
P. Wesseling, E. Oñate and J. Périaux (Eds)

HIGHER DIMENSIONAL NUMERICAL SIMULATIONS OF PRECIPITATE DISSOLUTION IN MULTI-COMPONENT ALUMINIUM ALLOYS

E. Javierre*, C. Vuik*, F.J. Vermolen*, A. Segal* and S. van der Zwaag†

*Delft University of Technology, Faculty EWI
Mekelweg 4, 2628 CD, The Netherlands
e-mail: e.javierreperez,c.vuik,f.j.vermolen,a.segal@tudelft.nl

†Delft University of Technology, Faculty L&R,
Kluyverweg 1, 2629 HS Delft, The Netherlands
e-mail: s.vanderzwaag@tudelft.nl

Key words: Particle dissolution, Vector-valued Stefan, Level Set Method

Abstract. *In thermal processing of alloys, homogenization of the as-cast microstructure by annealing at such a high temperature that unwanted precipitates are fully dissolved, is required to obtain a microstructure suited to undergo heavy plastic deformation. This process is governed by Fickian diffusion and can be modelled as a Stefan problem. In binary alloys[1], the interface concentration is the solid solubility predicted from thermodynamics. In multicomponent alloys, the interface concentrations should satisfy a hyperbolic equation and, therefore, have to be found as part of the solution. Geometrical reductions are normally taken in the numerical solution of vector-valued Stefan problems. The aim of this work is to extend a level set method[1] implemented for scalar Stefan problems, to higher dimensional vector-valued Stefan problems. This extension is obtained by adding a nonlinear coupling of the interface concentrations into the level set formulation. Computational results will be given for one-, two- and three-dimensional problems.*

1 INTRODUCTION

Heat treatment of metals is often used to optimize mechanical properties. During heat treatment, the metallurgical state of the alloy changes. This change can involve the phase present at a given location or the morphology of the various phases. Whereas equilibrium phases can be predicted quite accurately from thermodynamic models, there are no general models for microstructural changes nor for the kinetics of these changes. In the latter cases, both the initial morphology and the transformation mechanisms have to be prescribed explicitly. One of these processes, which is both of large industrial and scientific interest and amenable to modeling, is precipitate dissolution.

Several physical models have been developed to describe the dissolution of precipitates. The early models on particle dissolution, based on long-distance diffusion[2], consisted of analytic solutions in an unbounded medium under the assumption of local equilibrium at the interface. Nolfi[3] incorporates the interface reaction between the dissolving particle and its surrounding phase. Addition of secondary elements can influence the dissolution kinetics strongly[6]. Adding slower elements, i.e. elements with smaller diffusivities, will delay the dissolution process, whereas adding faster elements will make the dissolution process to proceed faster. Later modeling of particle dissolution has been extended to the introduction of multi-component particles[4,5]. In these papers, particle dissolution was viewed as a Stefan problem with a sharp interface separating the consecutive phases. When attempting to simulate particle dissolution in multi-component alloys, symmetry assumptions are used normally[5]. These assumptions are such that the problem can be reduced to one-spatial dimension. Our aim is to develop a numerical method capable of tackling dissolution of particles in multi-component alloys in higher dimensions.

Several numerical methods have been developed to solve Stefan problems. Front-tracking methods use an explicit representation of the interface, given by a set of points laying on the interface locations which should be updated at each time step. Juric and Tryggvason[7] combine a stationary mesh technique with a nonstationary curve or surface that represents the moving interface. Segal and co-workers[8] update the computational mesh, connected to the moving interface by a number of nodal points, each time step by means of an Arbitrary Lagrangian Eulerian (ALE) approach. Unfortunately, merging or breaking up of interfaces might become laborious to implement. Front-capturing methods use an implicit representation of the interface, adding an artificial unknown into the problem. Phase field methods[9] use a diffusive interfacial region, where the phase transformation occurs, and avoid applying explicitly the boundary conditions on the interface. Sharp interface problems are recovered in the limit on vanishing the interface thickness[10]. Adaptive mesh techniques[11,12] are needed in order to resolve the interface region accurately, which lead to small time steps. Level set methods[13] capture the interface as the zero level set of a continuous function, the so-called level set function. The motion of the interface follows from an advection equation for the level set function. The velocity field used for this advection should be a continuous extension of the front velocity[14,15].

In this work we first introduce the physical model for particle dissolution in multi-component alloys. Next, the level set method is described for vector-valued Stefan problems. A convenient extension of the front velocity onto the computational domain will be given, together with the iterative procedure to solve the coupled diffusion problems. After that, the numerical experiments will be presented, followed by the conclusions.

2 THE PHYSICAL PROBLEM

After manufacturing, an alloy is cast into a mould. The state of the alloy is then referred to as the as-cast state. The as-cast microstructure is simplified into a representative cell Ω containing a stoichiometric particle Ω_{part} with a given shape surrounded by a diffusive phase Ω_{dp} in which the alloy elements diffuse. The boundary between the particle and the diffusive phase is referred to as the interface Γ. Let p be the number of diffusive elements in the alloy. The particle dissolves due to Fickian diffusion in the diffusive phase

$$\frac{\partial c_i}{\partial t}(\mathbf{x},t) = D_i \Delta c_i(\mathbf{x},t), \quad \mathbf{x} \in \Omega_{dp}(t),\ t>0,\ i=1,\dots,p, \tag{1}$$

where D_i denotes the diffusion parameter of the ith alloying element. Cross-diffusion effects[16] have not been considered in the present work. Therefore, the classical diffusion equation is recovered for each element in the alloy. The particle is assumed to remain stoichiometric during the entire dissolution process. Hence, the particle concentrations remain constant

$$c_i(\mathbf{x},t) = c_i^{part}, \quad \mathbf{x} \in \Omega_{part}(t),\ t>0,\ i=1,\dots,p, \tag{2}$$

and the concentrations c_i^{sol} on the interface Γ satisfy the hyperbolic relation[17]

$$\prod_{i=1}^{p} \left(c_i^{sol}(\mathbf{x},t) \right)^{\tilde{n}_i} = \mathcal{K}(T), \quad \mathbf{x} \in \Gamma(t),\ t>0, \tag{3}$$

which has been derived from the Gibbs-free-energy of the stoichiometric elements, where the exponent $\tilde{n}_i$ denotes the stoichiometric number of the ith alloying element and $\mathcal{K}(T)$ denotes the solubility product which depends on temperature T. Since we consider an isothermal process, $\mathcal{K}(T)$ is a positive constant in our model. Note that the interface concentrations c_i^{sol} may depend on time and/or space, which represents a significant generalization of the dissolution models in binary alloys[1], where the interface concentration is the solid solubility from the binary phase diagram.

Mass conservation of all the alloying elements implies that

$$\left(c_i^{part} - c_i^{sol}(\mathbf{x},t)\right) v_n(\mathbf{x},t) = D_i \frac{\partial c_i}{\partial \mathbf{n}}(\mathbf{x},t), \quad \mathbf{x} \in \Gamma(t),\ t>0,\ i=1,\dots,p, \tag{4}$$

where v_n denotes the normal component of the interface velocity and $\mathbf{n}$ the unit normal vector on the interface pointing outward with respect to Ω_{part}. Note that Eqs. (4) implicitly impose that

$$\frac{D_i}{c_i^{part} - c_i^{sol}(\mathbf{x},t)} \frac{\partial c_i}{\partial \mathbf{n}}(\mathbf{x},t) = \frac{D_{i-1}}{c_{i-1}^{part} - c_{i-1}^{sol}(\mathbf{x},t)} \frac{\partial c_{i-1}}{\partial \mathbf{n}}(\mathbf{x},t), \quad \mathbf{x} \in \Gamma(t),\ t>0,\ i=2,\dots,p. \tag{5}$$

The above-formulated problem falls within the class of Stefan problems, i.e., diffusion with a moving interface. This problem is referred to as a vector-valued Stefan problem

since diffusion of several elements takes place simultaneously. The concentrations in the diffusive phase c_i, the interface position Γ and the interface concentrations c_i^{sol} are to be found. Note that p diffusion equations with coupled Dirichlet and Neumann interface conditions (3) and (5) need to be solved.

3 THE COMPUTATIONAL METHOD

The level set method is used to tackle the moving interface. Finite difference schemes are used to solve the hyperbolic equations inherited from the level set formulation, whereas a finite element method is used for the solution of the diffusion problems. For this purpose, a Cartesian mesh and a finite element triangulation are defined over Ω. Both meshes are based on the same nodal points so information is available everywhere with no need of interpolation. A similar method[18] has been applied recently to dendritic solidification.

3.1 The Level Set Method

The moving interface Γ is identified with the zero level set of a continuous function ϕ, the so-called level set function. Hence: $\phi(\mathbf{x},t)=0 \iff \mathbf{x}\in\Gamma(t)\ \forall t\geq 0$. Furthermore, ϕ is initialized as the signed distance function to the interface, being positive in Ω_{dp}. The motion of the interface is related to the level set function by

$$\frac{\partial\phi}{\partial t}(\mathbf{x},t)+\mathbf{v}(\mathbf{x},t)\cdot\nabla\phi(\mathbf{x},t)=0,\quad \mathbf{x}\in\Omega,\ t>0, \tag{6}$$

where $\mathbf{v}$ denotes a continuous extension of the front velocity onto Ω. On the moving interface we prescribe

$$\mathbf{v}(\mathbf{x},t)=\frac{D_1}{c_1^{part}-c_1^{sol}(\mathbf{x},t)}\nabla c_1(\mathbf{x},t),\quad \mathbf{x}\in\Gamma(t),\ t>0. \tag{7}$$

The Cartesian components of $\mathbf{v}$ are decoupled and extended independently by advection[14] in the proper upwind direction

$$\begin{cases} \frac{\partial v_k}{\partial\tau}+\mathrm{S}(\phi\phi_{x_k})\frac{\partial v_k}{\partial x_k}=0, & \\ v_k(\mathbf{x},0)=\frac{D_1}{c_1^{part}-c_1^{sol}(\mathbf{x},t)}\frac{\partial c}{\partial x_k}(\mathbf{x},t),\ \mathbf{x}\in\Gamma(t), & \text{for } k=1,2,3, \end{cases} \tag{8}$$

where $\tau>0$ denotes a pseudo-time and the notation $\mathbf{x}=(x_1,x_2,x_3)^t$ and $\mathbf{v}=(v_1,v_2,v_3)^t$ has been embraced.

After advecting the interface using Eq. (6), the level set function is, in general, not a distance function at the new time step. In order to prevent flat/steep gradients in the neighbourhood of the interface, the level set function is reinitialized[19] to a signed distance function in a band around the interface whenever it is necessary.

3.2 The diffusion problems

The diffusion equations (1) are solved with a standard Galerkin finite element method using linear elements. The underlying triangulation is adapted to the interface location each time step with the cut-cell method[1]. A temporary triangulation is created then, with additional nodes on the interface and additional subelements in the elements that where intersected by the interface. These extra nodes and elements are discarded, and hence the background mesh is recovered, after the coupled diffusion problems are solved.

The nonlinear coupling in the interface conditions Eqs. (3) and (5) is reformulated as the zero of a function $\mathbf{f} : \mathbb{R}^p_+ \to \mathbb{R}^p$ given by

$$\begin{cases} f_1(\mathbf{c}^{sol}) = \displaystyle\prod_{i=1}^{p} \left(c_i^{sol}\right)^{\tilde{n}_i} - \mathcal{K}(T) \\ f_i(\mathbf{c}^{sol}) = \dfrac{D_i}{c_i^{part} - c_i^{sol}} \dfrac{\partial c_i}{\partial \mathbf{n}} - \dfrac{D_{i-1}}{c_{i-1}^{part} - c_{i-1}^{sol}} \dfrac{\partial c_{i-1}}{\partial \mathbf{n}}, \ i = 2, \ldots, p \end{cases} \tag{9}$$

where the vectorial notation has been embraced for $\mathbf{c}^{sol}$. Note that $\mathbf{f}$ is defined on the interface, i.e. $\mathbf{c}^{sol} \equiv \mathbf{c}^{sol}(\mathbf{x}, t)$ along the interface points $\mathbf{x} \in \Gamma(t)$. A fixed-point iteration[20] is used to approximate the root of $\mathbf{f}$ on all the interface points up to a prescribed tolerance. Each iteration requires the simultaneous solution of p diffusion problems Eq. (1) with prescribed interface concentrations c_i^{sol}, the computation of the normal fluxes $\frac{\partial c_i}{\partial \mathbf{n}}$ along the interface and the update of $\mathbf{f}$.

4 NUMERICAL RESULTS

In this section we will give the results obtained with the numerical method presented above for a set of test problems. Comparison with self-similarity and the steady-state solutions will be carried out in the first test problem. In a second test, the evolution of the interface concentration c_1^{sol} will be studied for a two-dimensional problem. The last problem will deal with the dissolution of a three-dimensional cementite plate in a binary alloy, and will represent a more metallurgical problem. The other two problems will be more academic.

4.1 Comparison with the similarity solution

As a first test problem, we consider the dissolution of a planar interface. Because of the symmetry, this test problem is solved in one-spatial dimension only. We consider an alloy with three diffusional species, i.e. $p = 3$. The parameters of the problem are: the particle concentrations $\mathbf{c}^{part} = (5, 5, 5)$, the stoichiometric numbers $\tilde{\mathbf{n}} = (3, 1, 2)$, the diffusion coefficients $\mathbf{D} = (1, 2, 3)$, the length of the domain $L = 2.5$ and $\mathcal{K}(T) = 2$. Initially, the concentration of the diffusive species is uniform over the diffusive phase $\mathbf{c}^0 = (0, 0, 0)$, and the interface is located at $\Gamma(0) = 1.25$. The computational domain $\Omega = [0, L]$ is

split into $N = 100$ mesh intervals (i.e. $\Delta x_1 = \frac{L}{N}$). The evolution of the interface $\Gamma(t)$ and interface concentrations $c_i^{sol}(t)$ are plotted in Figure 1. The self similarity solution[5], defined in the unbounded domain, is used for comparison purposes. The evolution of the interface agrees with the similarity solution at the beginning of the dissolution process. At later stages of the dissolution, both curves diverge due to the boundedness of the computational domain. As time evolves, the interface position converges to the equilibrium position (i.e. steady-state) $\Gamma_\infty = 0.88815$. The interface concentrations agree, at $t = 0$, with those in the similarity solution. As time evolves they converge to the equilibrium values $c_{i,\infty}^{sol} = 1.1225$.

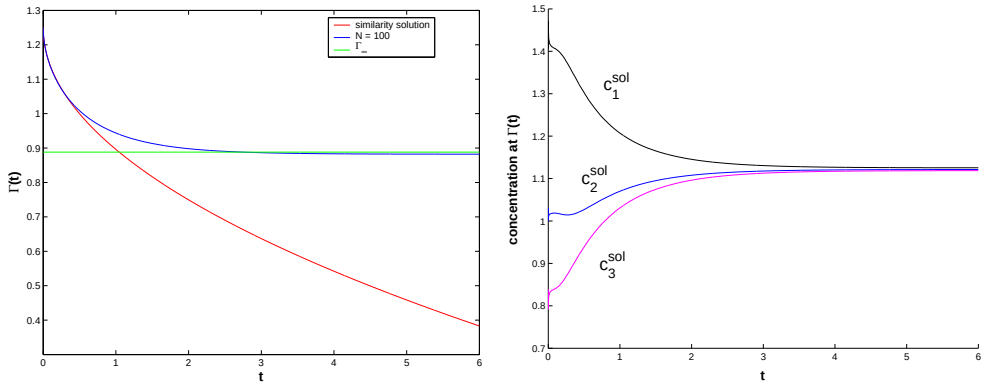

Figure 1: Planar interface.

4.2 Evolution of c_1^{sol} in a two-dimensional problem

As a second test case we consider the dissolution of a two-dimensional dumbbell-shaped particle. The number of diffusive species is $p = 2$. The parameters of the problems are: the particle concentrations $\mathbf{c}^{part} = (5, 5)$, the stoichiometric numbers $\tilde{\mathbf{n}} = (1, 1)$, the diffusion coefficients $\mathbf{D} = (1, 2)$, the initial concentration in the diffusive phase $\mathbf{c}^0 = (0, 0)$ and $\mathcal{K}(T) = 1$. The computational domain is $\Omega = [-0.5, 0.5]^2$ and the initial interface position is zero level set of $\phi^0(\mathbf{x}) = \min(\phi_{circ}(\mathbf{x}), \phi_{bar}(\mathbf{x}))$, where $\phi_{circ}(\mathbf{x}) = \min(\sqrt{(x_1 + 0.275)^2 + x_2^2} - 0.15, \sqrt{(x_1 - 0.21)^2 + x_2^2} - 0.2)$ corresponds to the exterior circles and $\phi_{bar}(\mathbf{x}) = \max(|x_1 + 0.0325| - 0.2425, |x_2| - 0.05)$ corresponds to the connecting bar. The mesh widths are $\Delta x_1 = \Delta x_2 = \frac{1}{50}$. Figure 2 shows the interface concentration of the first specie c_1^{sol} (red $\times$ marks) with the interface location (blue $\Diamond$ marks, which has been arbitrarily located at the plane $c_1^{sol} = 0.95$) at the beginning of the dissolution process. At the beginning, larger differences in c_1^{sol} are observed along the different parts (different geometries) of the interface. However, as time evolves, these differences are smeared out and already at $t = 0.024$ a nearly constant value of c_1^{sol} is observed along the interface. At later stages of the dissolution process, Figure 3, the

interface concentration c_1^{sol} remains constant along the interface, and monotonously decreases towards its equilibrium value $c_{1,\infty}^{sol} = 1$.

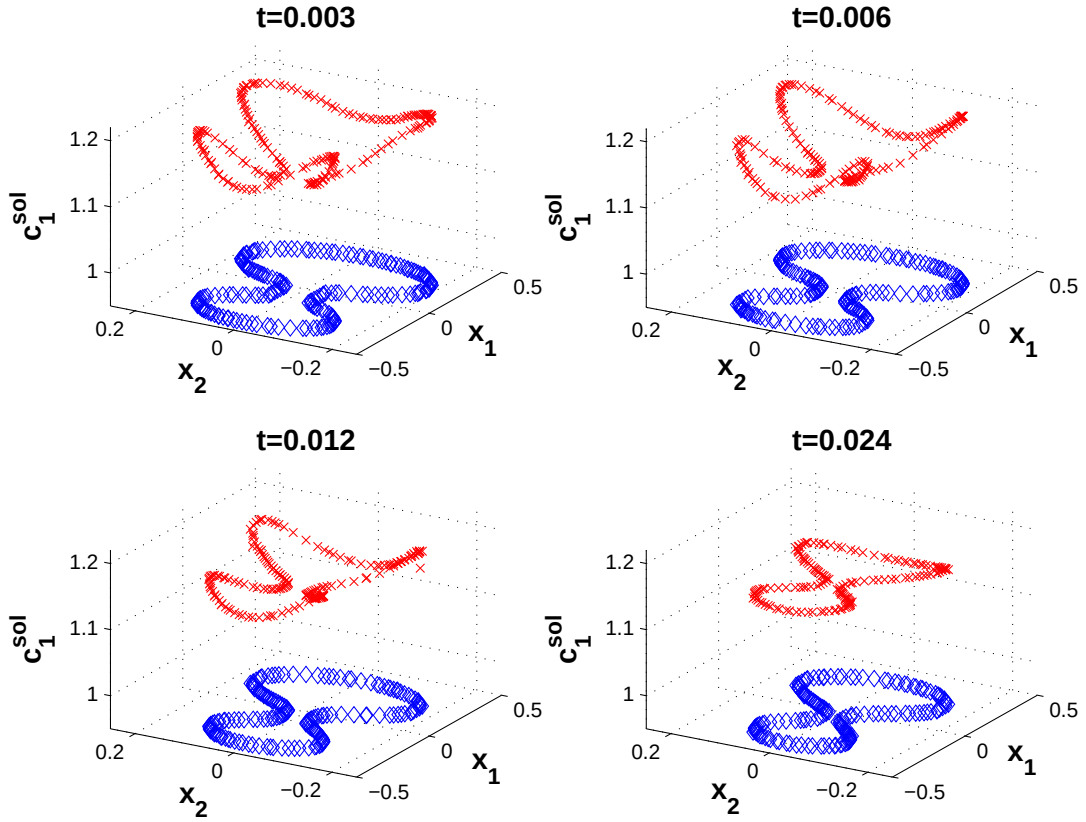

Figure 2: Interface position (blue ◊ marks) and c_1^{sol} (red × marks) at the beginning of the dissolution.

4.3 Dissolution of a cementite plate

As a final test problem we consider a three-dimensional cementite plate surrounded by a box-shaped ferrite matrix. Such a particle occurs often in a pearlite structure. The lamellae structure of pearlite is simplified into one cementite plate for reasons of symmetry. We assume a sinusoidal perturbation on the surface of the particle. Furthermore, we assume that the voids in the perturbed shape are filled by the ferrite phase entirely. The temperature has been chosen at $800^0\text{C} > A_1 = 727\ ^0\text{C}$ and the plate dimensions of $0.1 \times 1 \times 5\ \mu\text{m}^3$ have been used. The plate dissolves in a computational cell with dimensions $0.5 \times 2.4 \times 5\ \mu\text{m}^3$. Since our present three-dimensional model is not yet capable of dealing with three phases that occur simultaneously, which will be a future extension, it is assumed that the austenite-ferrite transformation occurs much faster than cementite dissolution. Hence the austenite-ferrite transformation is not considered here. This gives diffusion of

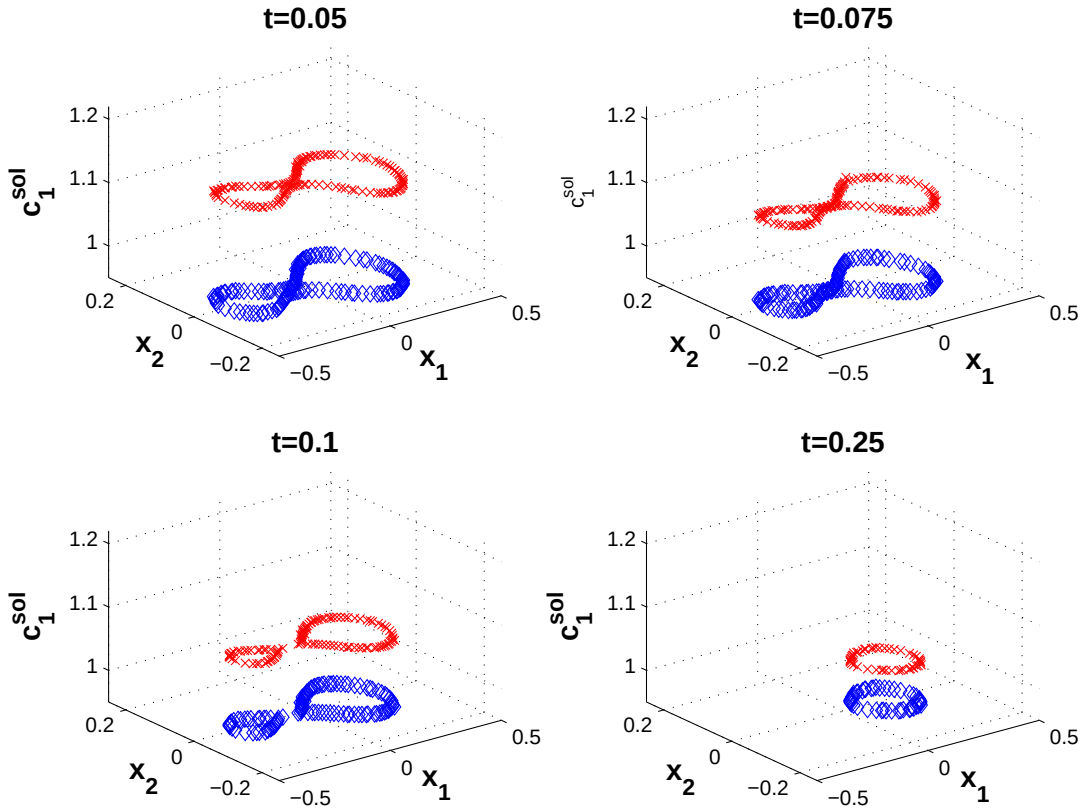

Figure 3: Interface position (blue $\Diamond$ marks) and c_1^{sol} (red $\times$ marks) at later stages of the dissolution process.

carbon in the austenite phase that surrounds the cementite particle. The concentration of carbon within the cementite particle is given by $c_C^{part} = 6.743$ wt. %. Further, the initial carbon composition in the austenite phase is set at $c_C^0 = 0$ wt. %. The concentration at the interface between the cementite and austenite phases is set equal to the value that follows from local equilibrium at $T = 800^0$C, given by $c_C^{sol} = 0.71719$ wt. %, during the entire dissolution process. For the diffusion coefficient the value $D_C = 2.98\ \mu m^2/s$ is used[21] (page 99), corresponding to the temperature of 800^0C. The results at consecutive times can be seen in Figure 4. It can be seen that the plate splits up into an array of dissolving rounded particles.

5 CONCLUSIONS

The dissolution of precipitates during heat treatments in alloys has been studied here. The physical problem has been modelled as a vector-valued Stefan problem, and the well known level set method has been used to follow the moving interface. The computational method for precipitate dissolution in binary alloys[1] has been extended here to multi-component alloys. Such an extension handles a nonlinear coupling of the interface

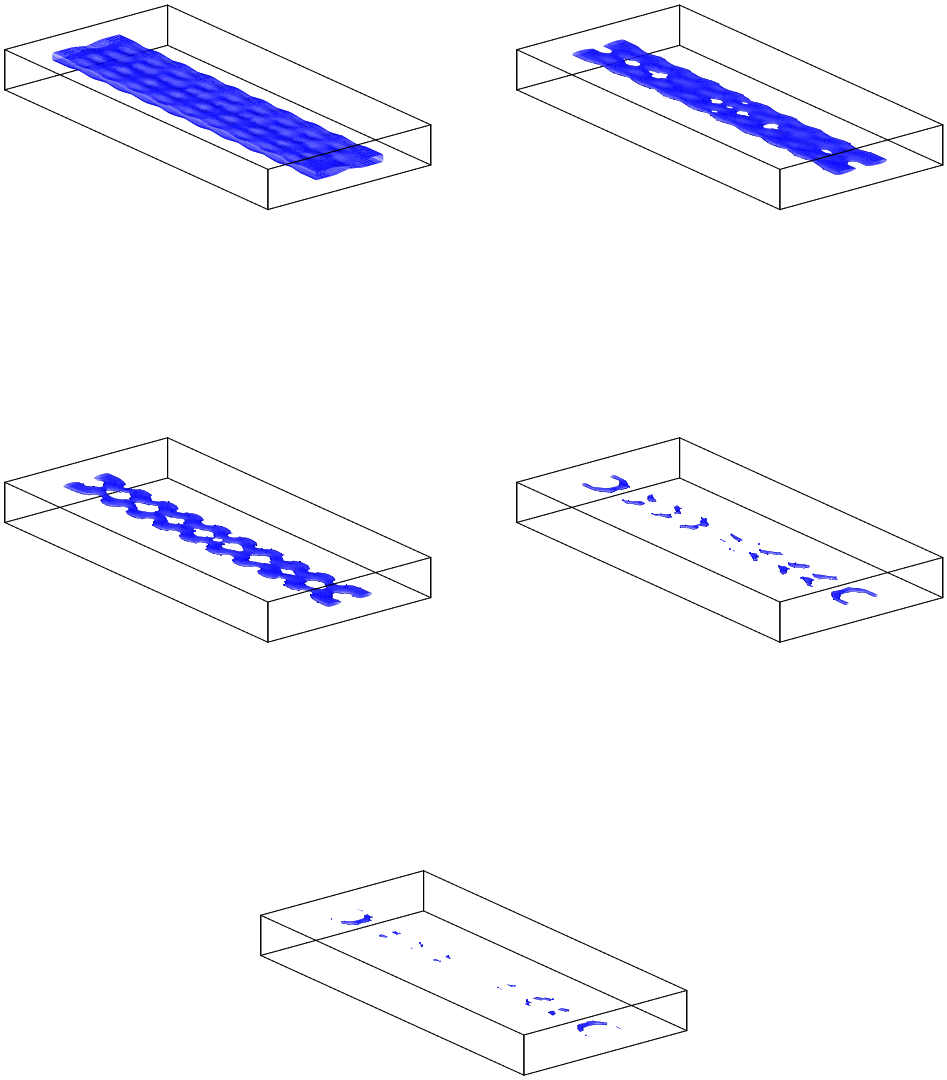

Figure 4: Dissolution of a cementite plate with a sinusoidal perturbation.

concentrations and concentration fluxes across the interface with a fixed-point iteration. This technique deals with breaking up of particles in a natural way, and is readily implemented in any spatial dimension. Numerical results have been given for one-, two- and three-dimensional problems. Agreement with similarity solutions and convergence to steady-state values have been obtained.

6 ACKNOWLEDGMENTS

This research is financially supported by the Dutch Technology Foundation (STW). The authors want to thank Dr. L. Zhao at the Materials Science and Engineering Dept. of the Delft University of Technology for addressing an interesting three-dimensional test problem that is relevant for the materials science community.

REFERENCES

[1] E. Javierre, C. Vuik, F.J. Vermolen and A. Segal. A level set method for particle dissolution in a binary alloy. *DIAM report 05-07*, Delft University of Technology, 2005.

[2] M.J. Whelan. On the kinetics of particle dissolution. *Metals Sci. J.*, **3**, 95–97, (1969).

[3] H.B. Aaron and G.R. Kotler. Second phase dissolution. *Metall. Trans.*, **2**, 393–407, (1971).

[4] J.-O. Andersson and J. Ågren. Models for numerical treatment of multicomponent diffusion in simple phases. *J. Appl. Phys.*, **72**, 1350–1355, (1981).

[5] F.J. Vermolen and C. Vuik. A mathematical model for the dissolution of particles in multi-component alloys. *J. Comp. and Appl. Math.*, **126**, 233–254, (2000).

[6] O. Reiso, N. Ryum and J. Strid. Melting and dissolution of secondary phase particles in AlMgSi-alloys. *Metall. Trans. A*, **24A**, 2629–2641, (1993).

[7] D. Juric and G. Tryggvason. A front-tracking method for dendritic solidification. *J. Comp. Phys.*, **123**, 127–148, (1996).

[8] G. Segal, K. Vuik and F. Vermolen. A conserving discretization for the free boundary in a two-dimensional Stefan problem. *J. Comp. Phys.*, *141*, 1–21, (1998).

[9] U. Grafe, B. Bötteger, J. Tiaden and S.G. Fries. Coupling of multicomponent thermodynamics to a phase field model: application to solidification and solid-state phase transformations. *Script. Mater.*, **42**, 1170–1186, (2000).

[10] G. Caginalp. Stefan and Hele-Shaw type models as asymptotics of the phase-field equations. *Phys. Rev. A*, **39**, 5887–5896, (1989).

[11] J.A. Mackenzie and M.L. Robertson. A Moving Mesh Method for the solution of the One-Dimensional Phase-Field Eequations. *J. Comp. Phys.*, **181**, 526–544, (2002).

[12] E. Burman, M. Picasso and J. Rappaz. Analysis and computation of dendritic growth in binary alloys using a phase-field model. *Numerical Mathematics and Advanced Applications*, Springer, (2004). 204–220.

[13] S. Osher and J.A. Sethian. Fronts propagating with curvature-dependent speed: Algorithms based on Hamilton-Jacobi formulations. *J. Comput. Phys.*, **79**, 12–49, (1988).

[14] S. Chen, B. Merriman, S. Osher and P. Smereka, A Simple Level Set Method for Solving Stefan Problems. *J. Comp. Phys.*, **135**, 8–29, (1997).

[15] F. Gibou, R. Fedkiw, R. Caflisch and S. Osher. A Level Set Approach for the Numerical Simulation of Dendritic Growth. *J. Sci. Comp.*, **19**, 183–199 (2003).

[16] F.J. Vermolen and C. Vuik. Solution of vector Stefan problems with cross-diffusion. *J. Comp. and Appl. Math.*, **176**, 179–201, (2005).

[17] F.J. Vermolen, C. Vuik and S. van der Zwaag. The dissolution of a stoichiometric second phase in ternary alloys: a numerical analysis. *Mater. Sci. Eng. A*, **246**, 93–103, (1998).

[18] L. Tan and N. Zabaras. A level set simulation of dendritic solidification with combined features of front-tracking and fixed-domain methods. *J. Comp. Phys.*, **211**, 36–63, (2006).

[19] D. Peng, B. Merriman, S. Osher, H. Zhao and M. Kang. A PDE-Based Fast Local Level Set Method. *J. Comput. Phys.*, **155**, 410–438, (1999).

[20] E. Javierre, C. Vuik, F. Vermolen, A. Segal and S. van der Zwaag. *Proceedings of ENUMATH 2005*, Springer-Verlag, to appear.

[21] W.D. Callister. *Materials science and engineering, an introduction*, John Wiley and Sons, New York, 4^{th} edition, (1997).